A Theoretical Study of Polarization Selective Two-Dimensional Vibronic Spectroscopies of Multimode Systems

Robert B. Weakly[1], James D. Gaynor[1,2], and Munira Khalil[1]
[1]*Department of Chemistry, University of Washington, Box 351700, Seattle, Washington, 98195, USA*
[2]*College of Chemistry, University of California, Berkeley, California, 94720, USA*
Email: mkhalil@uw.edu

Abstract: A model vibronic Hamiltonian composed of coupled anharmonic vibrational modes and two electronic states provides a quantitative framework for understanding how vibronic couplings and dipole orientations are encoded in two-dimensional vibronic spectroscopy.

Introduction: Two-Dimensional Electronic-Vibrational (2D EV) and Vibrational-Electronic (2D VE) spectroscopies are recent additions to the third-order nonlinear, Fourier Transform, multidimensional spectroscopy toolbox (Fig. 1) [1,2]. Combining the domains of 2D infrared (2D IR) and 2D electronic (2D ES) spectroscopies, 2D VE/EV directly interrogate the interplay and coupling between electronic states and vibrational modes and are uniquely sensitive to vibronic coupling in complex systems in the condensed phase [3]. Experimental manipulation of the polarization of three input fields allow for the determination of the angles between coupled electronic and vibrational dipoles and provides a mapping of vibronic coupling onto the molecular frame [4,5]. Extracting molecular level information from multimode polarization-selective 2D EV and 2D VE spectra is nontrivial. Here, we present a model Hamiltonian to study how signatures of vibronic couplings and the orientation of coupled vibrational and electronic degrees of freedom are encoded in the spectral features of polarization-selective 2D EV and 2D VE spectra.

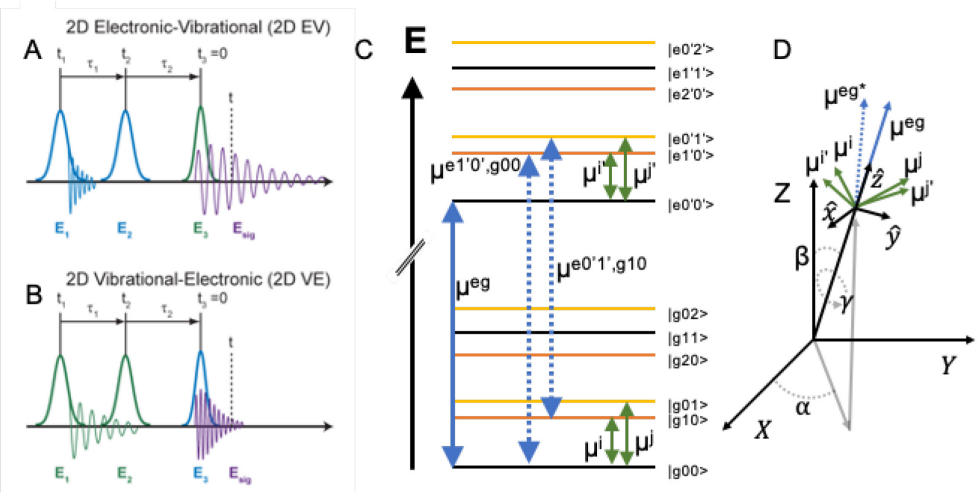

Fig. 1. **A:** 2D EV experimental pulse sequence. At t_1 a femtosecond optical (blue) pump pulse $\mathbf{E}_1$ is incident on the sample. At time t_2, after a coherence duration, τ_1, a second optical pump pulse $\mathbf{E}_2$ collapses the coherence or produces a new coherence between electronic states. This population (or new coherence) propagates during the waiting duration τ_2, until the infrared (green) probe pulse $\mathbf{E}_3$ interacts with the system to produce the third ordered signal field $\mathbf{E}_{sig}$, which can be collected over the time shown (t) via a local oscillator or via the probe pulse shown as t_3=0. **B:** VE experiments are performed with two infrared pump pulses and an optical probe pulse, initiating vibrational coherences and probing electronic transitions. **C:** Energy landscape, vibrational progressions of the ground and electronically excited states of a model molecule. States described as kets, g/e for the ground and electronically excited states, with values (0,1,2 | $0', 1', 2'$) to describe the quanta of excitation in the i^{th} and j^{th} mode. The ket $|e1'0'\rangle$ describes the excited electronic state and one quantum of vibrational energy in the i^{th} mode. Dipoles connect indicated states; vibrational dipoles (green) and electronic dipoles (blue). A separate dipole (blue dotted, μ^{eg*}) exists for each vibronic transition e.g. $\mu^{e1'0',g00}$. **D:** Molecular ($\hat{x}, \hat{y}, \hat{z}$), and laboratory frame (X,Y,Z), orientations of a model molecule. Shifts in vibrational character between ground and excited states determine each dipole vector's unique orientation within the molecular frame, which is aligned with the purely electronic transition dipole vector (μ^{eg}). Integrating over the Euler angles (α, β, γ) transforms the molecular frame into the laboratory frame. Polarization-selective experiments utilize pulses with varied polarizations in the laboratory frame to produce information about the molecular frame dipole orientations.

The model Hamiltonian is expanded from previous work [3], to include multiple coupled vibrational modes and is constructed as the sum of kinetic and potential energies of each mode. Equations (1) and (2) describe the potential of the ground (V_g) and excited states (V_e).

$$V_g(Q_i^0, Q_j^0) = \frac{\hbar\omega_i^0}{2}(Q_i^0)^2 + \frac{\hbar\omega_j^0}{2}(Q_j^0)^2 + B_{ij}Q_i^0Q_j^0 + \frac{1}{6}\left(\hbar\omega_i^0 g_{iii}(Q_i^0)^3 + \hbar\omega_j^0 g_{jjj}(Q_j^0)^3\right) \quad (1)$$

$$V_e(Q_i^0, Q_j^0) = V_g(Q_i^0, Q_j^0) + \hbar\omega_{eg}^0 + \hbar\omega_i^0 V_i Q_i^0 + \hbar\omega_j^0 V_j Q_j^0 + \frac{\hbar\omega_i^0}{2}V_{i,i}(Q_i^0)^2 + \frac{\hbar\omega_j^0}{2}V_{j,j}(Q_j^0)^2 + V_{i,j}Q_i^0Q_j^0 \quad (2)$$

The ground state potential is a function of displacement along the zeroth ordered vibrational coordinates (Q_i^0, Q_j^0) and approximates a harmonic oscillator with frequency (ω_i^0, ω_j^0) in each mode, cubic anharmonicity (g_{iii}/g_{ijj}) and bilinear vibrational mode mixing (B_{ij}). The excited state potential (V_e) is described by perturbations on the ground state potential and elevated by the electronic transition energy (ω_{eg}^0). Terms in the excited state potential are described by V_{xy} with subscripts denoting their coordinate dependence. V_i/V_j is a linear shift along each coordinate and its square is proportional to the Huang-Rhys factor [6]. V_{ii}/V_{jj} act to red/blue shift the potential along each coordinate. In the excited state, V_{ij} parallels the role that B_{ij} plays in the ground state, but is termed the Duschinsky mixing term [7], as it changes the character of the two electronic states relative to each other [8]. Diagonalization of this Hamiltonian produces the eigenstates described as energy levels in Fig. 1C and the transformation matrix is used to transform each vibrational dipole from the zeroth order dipole ($\hat{\mu}_i^0$) to the generalized dipole vectors ($\hat{\mu}^{a,b}$) [9], for transitions between arbitrary states (a) and (b), represented in Fig. 1D. This transformation gives rise to the vibronic orientational sensitivity of this model.

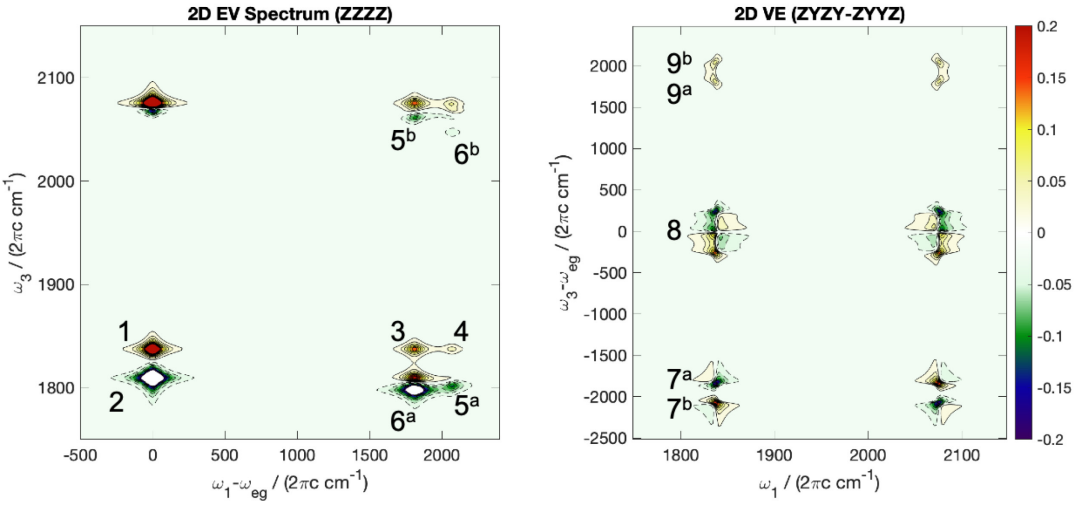

Fig. 2. 2D EV (left) and 2D VE (right) spectra of the same model system. Amplitude differences between ZZZZ and ZZYY spectra provide insight into the molecular orientation of each dipole moment assessed in the experiment. Peak convolution in VE spectroscopy limits the ω_3 resolution; the shown polarization combination (ZYZY-ZYYZ) isolates specific transitions. See text for details. All electronic axes are plotted relative to the ω_{eg}. The EV spectrum is normalized to its global maximum and the VE spectrum is normalized to 20% of its global maximum. Line shapes are determined by the electronic (Γ_{egeg}) and vibrational ($\Gamma_{x,v}$) frequency frequency correlation functions and state dependent dephasing rate (λ) in the homogeneous limit, as defined in earlier work [3,10]. Simulation parameters in cm^{-1}: $\omega_{eg}^0 = 16{,}500$; $\omega_i^0 = 1{,}850$; $\omega_j^0 = 2{,}100$; $B_{ij} = 0$; $g_{iii/jjj} = 330/490$; normalized to ~0.2 for each mode; $V_{i/j} = 827/664$; Huang-Rhys value: 0.1/0.05; $V_{ii/jj} = -10/-50$; $V_{ij} = -50$; $\Gamma_{egeg} = 40$; $\Gamma_{x,v} = 4$. State dependent dephasing rate: $\lambda_{i/j} = 1.0$. Zeroth ordered dipoles in the molecular frame: $\hat{\mu}^{eg} = \hat{z}$; $\hat{\mu}_i^o = \frac{1}{\sqrt{2}}(\hat{y} + \hat{z})$; $\hat{\mu}_i^o = \hat{z}$. Contours at 2% intervals between ± 0.20 to highlight spectral features.

Results: Fig. 2 displays polarization-selective 2D EV and 2D VE spectra using third-order nonlinear response theory [11], and Hamiltonian parameters listed in the figure caption. The peak positions, amplitudes and lineshapes encode the information contained in the vibronic Hamiltonian. For example, in the 2D EV spectrum, the energy splitting (24.6 cm^{-1}) of peaks 1 and 2 in ω_3 is the excited state energy difference in mode j, a result of V_{jj}. We note that splitting of the peak pair corresponding to mode i is much smaller, which is a direct consequence of the fact that $V_{jj} > V_{ii}$. Peaks 3 and 4 vary only in their electronic transition, gaining energy in mode i and j respectively. Comparing their amplitudes in the ZZZZ and ZZYY polarizations informs us about each mode's impact on the electronic dipole orientation. Peaks 5^a and 5^b each access the excited state mixed mode, probing the transitions $|e0'1'\rangle$ or $|e1'0'\rangle \rightarrow$

$|e1'1'\rangle$. This difference reports on the mixed mode anharmonicity (caused by Duschinsky mixing, Vij) in the electronically excited state. Measurement of the Duschinsky parameter (Vij) allow us to determine the extent of vibrational delocalization in the electronically excited state due to vibronic coupling. Further, peaks 6^a and 6^b probe the doubly excited vibrational manifold; their ω_3 positions indicating the excited state single mode anharmonicity.

Measurement of the parameters described above is limited by experimental resolution and more importantly, peak isolation. The polarization combination of VE spectroscopy shown in the right panel of Fig. 2 shows one of the ways polarization-selective experiments can aid in this endeavor. A τ_2 coherence in either spectroscopy forces the system to transition along four unique dipoles. This can be readily exploited to aid in peak deconvolution. For each transition pathway carrying a four-angle dependence, a pair of rephasing/non-rephasing peaks share the same dipoles but undergo transitions in a different order. The ZYZY/ZYYZ polarization schemes are sensitive to this difference in interaction sequence, but respond equally to all other peaks. Their difference highlights rephasing/non-rephasing mismatches and aids greatly in peak isolation. Two such pairs are easily seen at the bottom of the 2D VE (ZYZY-ZYYZ) spectrum in Fig. 2. The variety of electronic transitions probed by 2D VE spectroscopy allow interrogation of the dipole orientation of many vibronic transitions. For example, focusing on the right side of Fig. 2, we note that peaks 7 undergo the same electronic transitions and report angular information on both transitions which lose vibrational quanta, thus are lower in energy than ω_{eg}. Some peaks (not shown) in region 9, report on the orientation of the opposing transitions, which gain vibrational quanta. Peaks 9^a and 9^b, specifically, report on the excited state mixed mode transitions. Peaks 8 report directly on classically forbidden transitions like $\mu^{e0'1',g10}$ (Fig. 1D). The strength of these peaks is a result of both modes i and j forcing the transition dipole moment out of alignment with μ^{eg}.

Both 2D EV and 2D VE experiments report on the same molecular couplings between vibrations and electronic transitions manifested in different probes. 2D EV spectroscopy provides for direct interrogation of the excited state vibrational manifold, tracking those vibrations through any combination of excited states. 2D VE spectroscopy accesses more widely varied electronic transitions, reporting on how excited and ground state vibrations impact those transitions. The model described here provides a simple and consistent method for approaching these ultrafast polarization-selective experiments and all the data held therein.

Acknowledgements: The 2D EV simulations are supported by the National Science Foundation under Grant No. CHE- 1856413 and the 2D VE simulations are supported by the U.S. Department of Energy, Office of Science, Office of Basic Energy Sciences under Award Nos. DE-SC0019277. R.B.W. and J.D.G thank the NSF Graduate Research Fellowship Program for support under Grant No. (DGE-17621114).

References

[1] Oliver T.A.A., Lewis N.H.C., Flemming G.R. "Correlating the motion of electrons and nuclei with two-dimensional electronic-vibrational spectroscopy". P. Natl. Acad. Sci. USA **111**, 10061-10066 (2014).
[2] Courtney T.L., Fox Z.W., Slenkamp K.M., Khalil M. "Two-dimensional vibrational-electronic spectroscopy". J. Chem. Phys. **143**, 154201 (2015).
[3] Gaynor J.D., Khalil M. "Signatures of vibronic coupling in two-dimensional electronic-vibrational and vibrational-electronic spectroscopies". J. Chem. Phys. **147**, 094202 (2017).
[4] Fox Z.W., Blair T.J., Khalil M. "Determining the orientation and vibronic couplings between electronic and vibrational coordinates with polarization-selective 2D vibrational-electronic spectroscopy". J. Phys. Chem. Lett. **11**, 1558-1563 (2020).
[5] Gaynor J.D., Petrone A., Li X., Khalil M. "Mapping vibronic couplings in a solar dye with polarization-selective two-dimensional electronic-vibrational spectroscopy". J. Phys. Chem. Lett. **9**, 6289-6295 (2018).
[6] Huang K., Rhys A. "Theory of light absorption and non-radiative transitions in F-centers". Proc. R. Soc. Lond. A. **204**, 406-423 (1950).
[7] Tiwari V., Peters W., Jonas D.M. "Electronic energy transfer through non-adiabatic vibrational-electronic resonance. I. Theory of a dimer". J. Chem. Phys. **147**, 154308 (2017).
[8] Duschinsky F. "The importance of the electron spectrum in multi atomic molecules. Concerning the Frank-Condon principle". *Acta Physicochim Urs* **7**, 551-566 (1937).
[9] Golonzka O., Khalil M., Demirdöven N., Tokmakoff A. "Coupling and orientation between anharmonic vibrations characterized with two-dimensional infrared vibrational echo spectroscopy". **115**, 10814-10828 (2001).
[10] Sung J., Silbey R.J.. "Four-wave mixing spectroscopy for a multilevel system". J. Chem. Phys. **115**, 9266-9287 (2001).
[11] Mukamel S. *Principles of Nonlinear Optical Spectroscopy* (Oxford Union Press, New York, 1995).